

Ecosystem Services Assessment, Trade-Off and Bundles in the Yellow River Basin, China

Jie Yang (✉ 405899577@qq.com)

Gansu Agricultural University

Baopeng Xie

Gansu Agricultural University

Wenqian Tao

Gansu Agricultural University

Research Article

Keywords: Ecosystem service, Trade-off, Synergy, Ecosystem service bundles, Yellow River Basin

Posted Date: June 17th, 2021

DOI: <https://doi.org/10.21203/rs.3.rs-607828/v1>

License: © ⓘ This work is licensed under a Creative Commons Attribution 4.0 International License.

[Read Full License](#)

1 Ecosystem services assessment, trade-off and bundles in the
2 Yellow River Basin, China

3 Jie Yang¹ · Baopeng Xie² · Wenqian Tao²

4 ¹ College of Pratacultural Science, Gansu Agricultural University, Lanzhou 730070, China

5 ² College of Management, Gansu Agricultural University, Lanzhou 730070, China

6 ✉ Jie Yang e-mail:405899577@qq.com

7 **Abstract:**

8 Understanding ecosystem services (ESs) and their interactions will help to formulate effective
9 and sustainable land use management programs. This paper evaluates the water yield (WY), soil
10 conservation (SC), carbon storage (CS) and habitat quality (HQ), taking the Yellow River Basin as
11 the research object, by adopting the InVEST (Integrated Valuation of Ecosystem Services and
12 Trade Offs) model. The Net Primary Productivity (NPP) was evaluated by CASA
13 (Carnegie-Ames-Stanford approach) model, and the spatial distribution map of five ESs were
14 drawn, the correlation and bivariate spatial correlation were used to analyze the trade-off synergy
15 relationships between the five ESs and express them spatially. The results show that NPP and HQ,
16 CS and WY are trade-offs relationship, and other ecosystem services are synergistic. The trade-off
17 synergy shows obvious spatial heterogeneity. Driven by different factors, the leading ecological
18 function services in the Yellow River Basin can be divided into three areas, and WY and SC
19 service leading functional areas are mainly distributed in HQ and CS service leading functional
20 areas and NPP service leading functional areas. The results of functional bundles are obviously
21 affected by natural conditions such as land use/cover types and climate in the Yellow River Basin,
22 which can provide the basis for the Yellow River Basin to regulate ESs and maximize benefits.

23 **Keywords:** Ecosystem service, Trade-off, Synergy, Ecosystem service bundles, Yellow River
24 Basin

25 **1. Introduction**

26 ESs are the material basis and environmental conditions for the survival and development of
27 human, which can be divided into three categories: supply services, regulation services, and social
28 and cultural services. They are bridges to connect natural ecosystems and human well-being
29 (MEA,2005a). The sustainable supply is of great significance to the sustainable development of
30 districts, countries and even the whole world (Fu et al., 2014). In recent years, ESs have gradually
31 received attention in sustainable development research, and their definitions, classifications,
32 evaluations and driving mechanisms have been extensively studied (Costanza et al.,2017; Twenty
33 et al., 2017). The research focus has gradually shifted from the structure and process of
34 ecosystems to the relationship between human activities and ESs (Wu et al., 2019). Changes in
35 environmental factors such as land-use change and climate change will affect multiple ecological
36 processes such as the water cycle and carbon cycle, causing simultaneous changes in different ESs,
37 and different services may be related to the same ecological process, which ultimately leads to
38 complex connections between different ESs (Cord et al., 2017). The connections can be divided
39 into three categories: trade-off, synergy, and irrelevance. The trade-off relationship indicates that
40 the improvement of one service is accompanied by the decrease of another service; synergy
41 indicates that two services are increased or decreased at the same time, while irrelevance indicates
42 no significant connections between the temporal and spatial changes of the two services (Lyu et al.,
43 2018). The trade-off relationship analysis is of great significance in the management and
44 policy-making of ESs, and has gradually attracted the attention of researchers and has become a
45 hot research topic in related fields (Lyu et al., 2018). Mouchet, et al. (2014) reviewed and
46 quantitatively analyzed the main methods of exploring trade-off relationships in existing research.
47 Deng, et al. (2016) summarized the main tools and processes applied in the analysis of trade-off
48 relationships in land use management research. Howe, et al. (2014) conducted a comprehensive
49 analysis of how social-ecological environmental factors cause the trade-off relationship between
50 services. Richards et al. (2017) explored the trade-off relationship between ESs in tropical coastal

51 areas and future urban development, using the Pareto curve to analyze the trade-off and synergy
52 relationship between habitat quality and various ecological indicators. Trodahl et al. (2017)
53 studied the trade-off and synergy relationship between the water quality and agricultural
54 productivity of the fertile bay of New Zealand based on the LUCI module. Tolessa et al. (2017)
55 studied the impact of land use and land cover changes on ESs in the central highlands of Ethiopia
56 from 1973 to 2015, and the results showed that the reduction of forest coverage will lead to a
57 decrease in the value of ESs, which is mainly manifested in the ESs such as nutrient circulation,
58 raw material supply, and erosion control. Sun et al. (2019) used Yan'an City as the research area
59 and applied partial correlation analysis and found that there is a trade-off relationship between
60 food supply and soil conservation, water conservation and NPP, and there is a synergistic
61 relationship between NPP and soil conservation and water conservation, there is a synergistic
62 relationship between soil conservation and water conservation. Fu et al. (2016) studied ES
63 trade-offs and regional integration methods and analyzed the relationship between land use change
64 and ESs. Taking the Shiyang River Basin as an example, Wang Bei et al. used the InVEST model
65 and correlation coefficient method to study the trade-offs and synergies relationship among five
66 services, including water conservation, soil conservation, water purification, carbon storage, and
67 biodiversity (Wang et al., 2018). Many studies have achieved some achievements in the trade-offs
68 and synergy of ESs, but the researches on the regional differences and the driving factors in the
69 trade-offs and synergy relationship of ESs are still very inefficient. For example, the existing
70 studies mostly analyze natural environmental factors such as terrain and climate (Jiang et al.,
71 2016), ignoring the influence of social and economic development conditions (Zoderer et al.,
72 2016), even lacking comparative studies on the relative influence of different social-ecological
73 factors (Rositano et al., 2017), and lacking comprehensive analysis of driving forces and the
74 identification of dominant driving forces, consequently limit the application of research on ES
75 relationships in management practices.

76 Watershed is the best regional unit for studying ESs (Cheng et al., 2015), which has a variety
77 of service types. Under the combined effect of social and ecological factors, ESs exhibit complex
78 Spatio-temporal relationships. At the same time, the river basin is also one of the areas with the

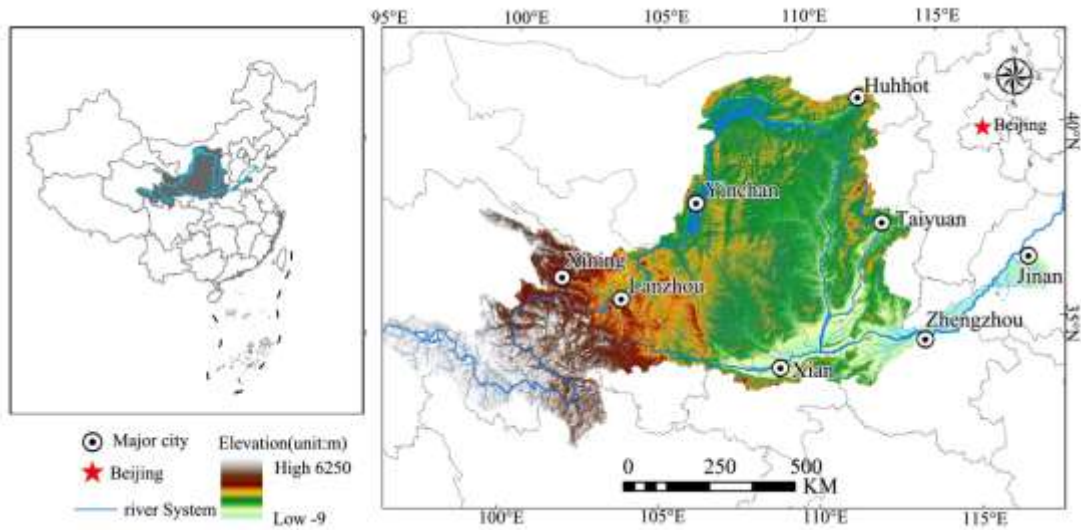
79 strongest disturbance to human activities. It is faced with water quality degradation, insufficient
80 water supply, soil erosion, and degradation of habitat quality. How to coordinate economic
81 development and environmental protection and alleviate conflicts between upstream and
82 downstream stakeholders becomes the key to the sustainable development of the basin. ESs are an
83 important link to connect the natural environment and human needs. By studying the trade-offs
84 and synergy relationship of various ESs in the River basin, and clarifying its driving mechanism, it
85 is helpful to formulate the “win-win” policy measures for the River basin development and
86 ecological protection (Li et al., 2016; Liu et al., 2019). The Yellow River Basin is a vast area
87 located in northwestern of China. It spans from the east to the west and has the characteristics of
88 complex geomorphic units, diversified ecosystem types, and obvious regional climate differences.
89 Its ecosystem environment is fragile and is one of the sensitive regions of global climate change
90 (Chen et al.,). The Yellow River Basin constitutes an important ecological barrier in our country, is
91 an ecological corridor connecting the Qinghai-Tibet Plateau, the Loess Plateau and the North
92 China Plain, which has multiple geographical units such as the source of the Three Rivers, Qilian
93 Mountains, Hetao Plain, and Huanghuaihai Plain. There are important areas with ecological
94 functions such as water conservation, wind protection, sand fixation, and biological diversity
95 protection, which play a very significant role in maintaining regional ecological security.

96 Based on this, this study takes the year 2018 as a cross-section to analyze the spatial
97 trade-offs among the five ESs and their association with social ecosystems. First, it quantitatively
98 calculates the spatial distribution pattern of WY, CS, SC, HQ, and NPP, calculates the correlation
99 coefficient between ESs through correlation analysis and uses SOM to classify the spatial
100 distribution of ESs clusters. Then the random forest model is used to explore the impact of
101 social-ecological influencing factors on ESs, and the SOM method is used to classify the clusters
102 of social-ecological factors. Finally, it distinguishes the relationship between ES clustering and
103 social-ecological factor clustering through overlay analysis, to explore the response mechanism of
104 ESs to the social-ecological system. It is expected to lay the foundation for the ecology and
105 environmental protection of the basin.

106 **2. Study area**

107 The Yellow River originates from the Yogu Zonlie Basin at the northern foot of the Bayan
108 Har Mountain on the Qinghai-Tibet Plateau. It flows through Qinghai, Sichuan, Gansu, Ningxia,
109 Inner Mongolia, Shanxi, Shaanxi, Henan, and Shandong provinces, and injects into the Bohai Sea
110 in Kenli County, Shandong Province. The main stream has a total length of 5464 kilometers and a
111 drop of 4480 meters(Fig.1). The Yellow River Basin is located between 96° - 119° east longitude
112 and 32° - 42° north latitude, with a length of about 1,900 kilometers from the east to the west
113 and a width of about 1,100 kilometers from the north to the south. The area of the basin is 795,000
114 square kilometers (including the internal flow area of 42,000 square kilometers). Above Hekou
115 Town, it is the upper reaches of the Yellow River, with a river course of 3,472 kilometers and a
116 basin area of 428,000 square kilometers; from Hekou Town to Taohuayu, it is the middle reaches,
117 with a river course of 1,206 kilometers and a basin area of 344,000 square kilometers; below
118 Taohuayu, it is the lower reaches, with a river course of 786 kilometers and a basin area of only
119 23,000 square kilometers. In the Yellow River Basin, there is a vast area, numerous mountains,
120 great differences in height between the east and the west, and great differences in landforms
121 between regions. The climate of different regions in the basin differs significantly. In the Yellow
122 River Basin, the sunlight is sufficient and the solar radiation is strong, and the sunshine conditions
123 belong to sufficient areas across the country. The annual sunshine hours generally reach
124 2000-3300 hours. There are big seasonal differences in the Yellow River Basin. The annual
125 precipitation in most areas of the basin is between 200 and 650 mm, and that of the upper reaches
126 of the southern and lower reaches is more than 650 mm, especially the northern slope of the
127 Qinling Mountains in the south, which is heavily affected by topography. Generally, it can reach
128 700-1000 mm, and it gradually increases from the northwest to the southeast. The precipitation is

129 unevenly distributed, and the ratio of rainfall between the north and the south is greater than 5.
 130 According to the national water resources distribution, the Yellow River basin can be divided into
 131 8 secondary basins and 29 tertiary basins.



132
 133

Fig.1 Range of Yellow River Basin and distribution of river system

134 3. Data and Methodology

135 3.1 Data sources

136 In this study, we use multi-source data sets to evaluate ESs in space, including land use/cover
 137 data sets, satellite image data sets, meteorological data sets, soil data sets, statistical data sets and
 138 related auxiliary data sets. Detailed descriptions of data sources are shown in Table 1.

139 Tab.1 Summary of main data types and data sources

ES	Data requirement type	Unit	Data sources
	Precipitation	mm	Geographic Data Cloud of Chinese Academy of Sciences The Data Set of Global Potential
WY	Potential evapotranspiration	mm	Evapotranspiration and Global Drought Index
	Soil texture	int	HWSD Soil Database
	Available water content of plant	%	Generated from soil texture data

	Land use/cover type	int	Geographical national conditions monitoring cloud platform
	Catchment area/sub-catchment area distribution	int	DEM data generation
	Root depth of plant	mm	1:1 million soil database of China
	Evapotranspiration coefficient	—	Food and Agriculture Organization of the United Nations, 1998
CS	Land use / cover type	int	Geographical national conditions monitoring cloud platform
	Carbon density data of various land use types	t/hm ²	InVEST model, references
	DEM	m	Geospatial Data Cloud
	Rainfall erosivity	MJ·mm/(hm ² ·h·a)	Calculation based on rainfall data
	Soil erodibility factor	t·hm ² /(MJ·mm)	Calculation based on soil texture data
SC	Land use /cover type	int	Geographical national conditions monitoring cloud platform
	Catchment area/sub-catchment area distribution map	int	DEM data generation
	Vegetation Management Factor	—	Calculation based on NDVI data
	Engineering measures factor	—	references
HQ	Land use/ cover type	int	Geographical national conditions monitoring cloud platform
	Major threats	—	InVEST model, references
	The weight of threat source factor	—	InVEST model, references
	Sensitivity of various land use types to stress factors	—	InVEST model, references
NPP	Land use /cover type	int	Geographical national conditions monitoring cloud platform
	NDVI	int	Earth resources observation and science center
	Meteorological data	int	Geographical national conditions monitoring cloud platform

140 3.2 ES quantification and mapping

141 Considering the characteristics of the ecological environment of the Yellow River Basin and
142 the availability of data, combining the characteristics of natural geography and social economy,
143 five more important ESs are selected from the ESs, namely NPP, WY, CS, SC and HQ.

144 3.2.1 Net Primary Productivity (NPP)

145 NPP refers to the production capacity of green vegetation, which is an important parameter of
146 the ecosystem carbon cycle and energy flow. This study evaluates the NPP of the Yellow River
147 Basin by adopting the CASA model and ENVI remote sensing estimation module. This method
148 has simple parameters and takes the impact of vegetation classification on the assessment results
149 into account, due to the availability of the parameters and the simplicity of operation of the model
150 that have been widely used in the estimation of NPP. The calculation formula of this method is:

151
$$NPP = APAR \times \varepsilon \quad (1)$$

152
$$APAR = SOL \times FPAR \times 0.5 \quad (2)$$

153
$$FPAR = \min\left[\frac{SR - SR_{min}}{SR_{max} - SR_{min}}, 0.95\right] \quad (3)$$

154
$$SR = \left[\frac{1 + NDVI}{1 - NDVI}\right] \quad (4)$$

155
$$\varepsilon = T_{\varepsilon 1} \times T_{\varepsilon 2} \times W_{\varepsilon} \times \varepsilon_{max} \quad (5)$$

156 In the formula, NPP, APAP, ε respectively represent the net primary productivity of
157 vegetation ($g \cdot c \cdot m^{-2}$), the absorbed photosynthetically active radiation ($MJ \cdot m^{-2}$) and the actual light
158 utilization rate ($g \cdot c \cdot MJ^{-1}$). SOL and FPAR are respectively the total solar radiation ($MJ \cdot m^{-2}$) and
159 the absorption ratio of photosynthetically active radiation by vegetation; the constant 0.5
160 represents the solar radiation rate used by vegetation; SR_{min} is 1.08, and SR_{max} is related to
161 vegetation types. NDVI represents vegetation coverage; $T_{\varepsilon 1}$, $T_{\varepsilon 2}$ and W_{ε} are the threat effects of

162 low temperature, high temperature, and moisture conditions on the light utilization efficiency. For
 163 specific algorithms, please refer to Piao et al. (2001), Zhu et al. (2005a, 2005b) and Mu et
 164 al.(2013).

165 3.2.1 Water yield (WY)

166 This study evaluates the water yield by adopting the InVEST model water production module,
 167 which is based on the Budyko water-heat coupling balance hypothesis and the annual average
 168 precipitation data, that is, the rainfall of each grid minus the actual evapotranspiration is the
 169 annual water production $Y(x)$ of each grid unit x in the study area (Sharp et al., 2018), the
 170 calculation formula is:

$$171 \quad Y_{xj} = \left(1 - \frac{AET_x}{P_x}\right) \times P_x \quad (6)$$

$$172 \quad \frac{AET_x}{P_x} = \frac{1+w_x R_x}{1+w_x R_{xj} + \frac{1}{R_x}} \quad (7)$$

$$173 \quad w_x = Z \times \left(\frac{AWC_x}{P_x}\right) \quad (8)$$

$$174 \quad R_x = \frac{k_x \times ET_{ox}}{P_x} \quad (9)$$

$$175 \quad AWC_x = \text{Min}(MSD_x, RD_x) \times PAWC_x \quad (10)$$

176 In the formula, Y_x is the average annual water production of grid x . Since the actual annual
 177 evapotranspiration cannot be directly measured and obtained, the curve pair AET_x/P_x can be used
 178 to approximate calculations. The R_x value is dimensionless and is the dryness index of grid x . It
 179 can be calculated by potential evapotranspiration and rainfall. w_x is an empirical parameter used to
 180 describe climate-soil properties, and can be calculated by the available water content of vegetation
 181 and annual rainfall. AWC_x is the available water content of vegetation, which is determined by soil
 182 texture and effective soil depth and is used to determine the total amount of water stored and
 183 provided by the soil for plant growth. Z is called the Zhang coefficient (Zhang et al., 2001), which

184 is an empirical constant, which represents the parameters of seasonal rainfall distribution and
185 rainfall depth. For areas dominated by winter rainfall, the Z value is close to 10, while for humid
186 areas where rainfall is evenly distributed and areas dominated by summer rainfall, the Z value is
187 close to 1. According to the results of multiple simulations, the Z value is finally determined to be
188 3.6. ET_{0x} is the internal potential evapotranspiration in grid x , which reflects the
189 evapotranspiration capacity determined by weather and climate conditions. Since the data of
190 potential evapotranspiration are difficult to obtain, so they are usually calculated by the
191 temperature method, the radiation method and the comprehensive method. InVEST model uses the
192 Modified-Hargreaves method to calculate the potential evapotranspiration. k_x represents the
193 evapotranspiration coefficient of vegetation or crops, and there are different evapotranspiration
194 coefficients for different land use types. MSD_x (Max Soil Depth x) is the maximum soil depth. RD_x
195 is the root depth. $PAWC$ is the available moisture content of plants. Please refer to (Yang et al.,
196 2020) for the calculation of specific parameters.

197 3.2.2 Carbon Storage (CS)

198 This paper divides the carbon storage of the ecosystem into four basic carbon pools by using
199 the InVEST model carbon storage module. They are respectively: the above-ground biological
200 carbon (carbon in all living plant materials above the soil), the underground biological carbon
201 (carbon presents in the living root system of plants), the soil carbon (organic carbon distributed in
202 organic soil and mineral soil), and the dead organic carbon (carbon in litter, upside-down or
203 standing dead trees). The carbon module of the model takes each land use type as the evaluation
204 unit and multiplies the average density of the four carbon pools by the area of each evaluation unit
205 to calculate the carbon storage of the study area. The calculation formula for the total carbon

206 density of each land-use type is as follows:

$$207 \quad C_{\text{tot}} = C_{\text{above}} + C_{\text{below}} + C_{\text{soil}} + C_{\text{dead}} \quad (11)$$

208 In the formula: C_{tot} is the total carbon storage ($\text{t}\cdot\text{hm}^{-2}$). C_{above} , C_{below} , C_{soil} , C_{dead} are the
209 above-ground biological carbon storage ($\text{t}\cdot\text{hm}^{-2}$), the underground biological carbon storage
210 ($\text{t}\cdot\text{hm}^{-2}$), the soil carbon storage ($\text{t}\cdot\text{hm}^{-2}$), and the dead organic carbon storage ($\text{t}\cdot\text{hm}^{-2}$).

211 Based on the carbon density and land use data of various regions, the formula for calculating
212 the carbon storage of the ecosystem in the basin is as follows:

$$213 \quad C_{\text{tot}i} = (C_{\text{ai}} + C_{\text{bi}} + C_{\text{si}} + C_{\text{di}}) \times A_i \quad (12)$$

214 Where: i is the average carbon density of each land use type. A_i is the area of the land-use
215 type. Please mainly refer to related studies (Xie et al., 2004; Li et al., 2003; Chen et al., 2002;
216 Chuai et al., 2013) for the carbon density data in the carbon pool table required for the model.
217 According to regional similarity, the desirability of results, and other principles, it can generate a
218 carbon pool table.

219 3.2.3 Soil Conservation (SC)

220 In this paper, the amount of soil conservation includes two parts: the amount of erosion
221 reduction and the amount of sediment interception based on the calculating principle of the soil
222 conservation module in the InVEST model. The former refers to the reduction of potential erosion
223 land of each block, expressed as the potential erosion and actual erosion difference. The latter
224 refers to the retention of sediment from the upslope by the block, which is expressed as the
225 product of the amount of sediment and the efficiency of sediment retention. The model calculation
226 formula is as follows:

$$227 \quad SEDRET_x = RKLS_x - USLE_x + SEDR_x \quad (13)$$

228
$$RKLS_x = R_x \times K_x \times LS_x \quad (14)$$

229
$$USLE_x = R_x \times K_x \times LS_x \times P_x \times C_x \quad (15)$$

230
$$SEDR_x = SE_x \sum_{y=1}^{x-1} USLE_y \prod_{z=y+1}^{x-1} (1 - SE_z) \quad (16)$$

231 In the formula: $SEDRET_x$, $RKLS_x$, $USLE_x$, $SEDR_x$ and $USLE_y$ are respectively the soil
 232 conservation amount of grid x , the potential soil erosion amount, the actual erosion amount after
 233 considering management and engineering measures, the sediment retention amount, and the actual
 234 erosion amount of the upslope grid y after considering management and engineering measures,
 235 which are all in units of t. R_x , K_x , LS_x , C_x , and P_x are the precipitation erodibility factor, soil
 236 erodibility factor, slope length factor, vegetation cover management factor, and soil and water
 237 conservation measures factor of grid x , respectively. Please refer to (Liu et al., 2018) for the
 238 calculation process of each factor.

239 3.2.4 Habitat Quality (HQ)

240 In the InVEST model, the Habitat Quality model evaluates the quality of the habitat.
 241 The model calculates the negative impact of threatening factors on the habitat, and obtains
 242 the degradation degree of the habitat, by establishing the connection between land use data
 243 and threat factors, and comprehensively considering factors such as the distance and intensity
 244 of threat factors. Then it calculates the quality of the habitat through the degradation degree
 245 and habitat suitability to reflect the biodiversity of the area (Bao et al., 2015). The calculation
 246 formula is:

247
$$Q_{xj} = H_j \left(1 - \left(\frac{D_{xj}^z}{D_{xj}^z + k^z} \right) \right)$$

248 In the formula: Q_{xj} is equal to the habitat quality index of grid x in land use j . H_j refers to the
 249 habitat suitability of habitat type j , with a value range of 0-1. D_{xj} refers to the habitat degradation

250 index. R is the number of threat factors. k is the half-saturation constant, which is generally 1/2 of
 251 the maximum value of habitat degradation. z is the normalized constant, which is usually set to 2.5
 252 (Sharp et al., 2018).

253 The parameters that need to be input in this module mainly include land-use type maps,
 254 main habitat threat factors, weights of threat source factor and influence distances, and data such
 255 as the sensitivity degree of land use types to threat sources, etc. These research results are set after
 256 taking reference to the InVEST model manual (Sharp et al., 2014), the scholars' research results
 257 (Zhong et al., 2017; Liu et al., 2017; Zhang et al., 2020) and experts' suggestions.

258 3.3 Trade-offs, synergy, and bundle analysis among ESs

259 3.3.1 Correlation analysis

260 Correlation analysis can effectively reflect the direction and degree of the changing trend
 261 between two variables (Hou et al., 2017). The commonly used correlation coefficients are Pearson
 262 coefficient, Spearman coefficient, and Kendall coefficient. The Spearman rank correlation
 263 coefficient mainly performs the linear correlation analysis by using the rank size, and it doesn't
 264 require the distribution of the original variables. It is a non-parametric statistic method (Hu et al.,
 265 2015), and has lower requirements on the original data (Li et al., 2017). The overall distribution
 266 pattern or sample size is not required. As long as the observation values of the two variables are
 267 paired with each other, the coefficient can be used for calculation, and even the grade data
 268 converted from continuous variables can be analyzed. The scope of application is very wide (Ying
 269 er al., 2020).

$$270 P_{X,Y} = \frac{cov(X,Y)}{\sigma_X\sigma_Y} = \frac{E((X - \mu_X)(Y - \mu_Y))}{\sigma_X\sigma_Y} = \frac{E(XY) - E(X)E(Y)}{\sqrt{E(X^2) - E^2(X)}\sqrt{E(Y^2) - E^2(Y)}}$$

$$271 r_g = P_{rgX,rgY} = \frac{cov(rgX,rgY)}{\sigma_{rgX}\sigma_{rgY}}$$

272

273 In the formula, $P_{X,Y}$ is the Pearson correlation coefficient of variables X and Y. $cov(X, Y)$ is
274 the covariance of the two variables. σ_X and σ_Y are the standard deviation of the two variables.
275 $P_{rgX,rgY}$ is the Spearman correlation coefficient, which is applied to the rank of the original
276 variable.

277 Based on the correlation analysis function of the R language, this research explores the
278 trade-offs and synergy among the five ESs of NPP, WY, CS, SC, and HQ. The pie chart shows the
279 correlation between the service function of ESs. Blue means positive correlation, red means
280 negative correlation. The darker the color, the greater the correlation between the two variables.
281 The meaning of the color of the upper triangular cell in the figure is the same as that of the lower
282 triangular cell, but the degree of correlation is expressed by the filled area of the graph chart in the
283 pie. The greater the correlation, the more the filled area. The positive correlation fills the pie chart
284 clockwise from 12 o'clock, and the negative correlation fills the pie chart counterclockwise.

285 3.3.2 Global spatial autocorrelation

286 Moran's I index shows the similarity ratio of unit attribute values in the spatial adjacent areas.
287 In this paper, it analyzed the spatial correlation between water yield and rainfall of each grid cell
288 in the Yellow River Basin by GeoDA. The formula is in the following:

$$289 I = \frac{n \sum_{i=1}^n \sum_{j=1}^n w_{ij} (x_i - \bar{x})(x_j - \bar{x})}{\sum_{i=1}^n (x_i - \bar{x})^2 (\sum_i \sum_j w_{ij})}$$

$$290 Z(G_i^*)$$

$$291 = \frac{\sum_{j=1}^n w_{ij} x_j - X \sum_{j=1}^n w_{ij}}{\sqrt{\frac{[n \sum_{j=1}^n w_{ij}^2 - (\sum_{j=1}^n w_{ij})^2]}{(n-1)}}}$$

$$292 X = \frac{1}{n} \sum_{j=1}^n x_j, \quad S = \sqrt{\frac{1}{n} \sum_{j=1}^n x_j^2 - x^2}$$

293 In the formula: I is Moran's I index, n is spatial cells' number; x_i and x_j are respectively
294 the observed values of i and j regions; w_{ij} is the spatial adjacency relationship of regions i
295 and j ; S^2 is the variance of observed values. The Moran's I index is generally between - 1 and 1.
296 [0,1] indicating that the geographical entities have a positive correlation, and [- 1,0] shows a
297 negative correlation, and the value of 0 indicates there is no correlation.

298 3.3.3 Principal component analysis

299 Principal Component Analysis (PCA) is a method of mathematical transformation, which
300 converts a given set of related variables into another set of unrelated variables which are arranged
301 in descending order based on variance through linear transformation. In the mathematical
302 transformation, the total variance of the variable is unchanged, so that in the first variable, there is
303 the largest variance called the first principal component, and in the second variable, there is the
304 second-largest variance and has no relation with the first variable, which is considered as the
305 second principal component. By analogy, one variable has one principal component. The steps are
306 as follows: 1) Standardization of multivariate data; 2) Determination of correlation between
307 variables; 3) Determination of the number of principal components; 4) Obtaining of the principal
308 components.

309 3.3.4 SOM method

310 The SOM is an unsupervised neural network method based on competitive learning
311 (Kohonen et al., 1989). It is composed of an input layer and an output layer (also called a
312 competition layer). The input layer is used to receive input training samples, and the neurons in
313 the output layer are generally arranged in a two-dimensional array, and each neuron in the two
314 layers is bidirectionally connected. The SOM classifies the set of input patterns by finding the

315 optimal weight vector, that is, the best matching neuron. The steps of the SOM algorithm are:
316 initializing each weight vector, that is, assigning small random numbers to each weight vector in
317 the output layer and normalize it; finding the winning neuron of the input data; adjusting the
318 weight vector in the winning neighborhood; repeatedly searching for the input data of the winning
319 neuron and subsequent steps until the iteration termination condition is met.

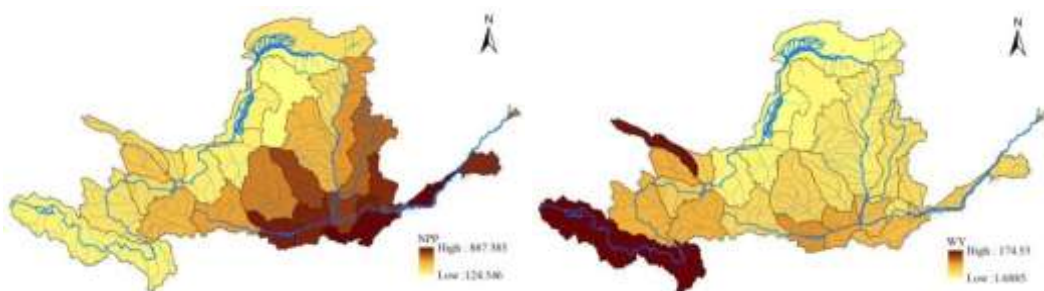
320 **4. Results and Analysis**

321 4.1 ESs and their spatial distribution characteristics

322 In 2018, the five ESs of NPP, WY, CS, SC and HQ in the Yellow River Basin were
323 $336.99\text{gc}\cdot\text{m}^{-2}$, $451.695\times 10^8\text{m}^3$, $15.4685\times 10^6\text{t}$, $78.4265\times 10^8\text{t}$ and 0.684, respectively. The five
324 ESs functions studied in this study are calculated and displayed on the map. They are unevenly
325 distributed (Fig. 2). The areas with high NPP values are distributed mainly in the lower reaches in
326 the Yellow River, including the Weihe-Guanzhong Basin, Fenhe River Basin, as well as the area
327 below Huayuankou. The low-value areas are mainly distributed in the middle reaches of the
328 Yellow River Basin, including the Lanzhou to Hekouzhen watershed etc, showing a zonal pattern
329 of high in the east and low in the west. WY shows the highest water production in the upper
330 reaches of the Yellow River, such as areas of Longyangxia and above. This area has more ice and
331 snow melt water replenishment, higher vegetation coverage, and low evapotranspiration. It is the
332 main source of runoff in the Yellow River Basin, and the main stream has a large runoff. The basin
333 from Lanzhou to Hekou Town is the low-value area of WY. The evaporation in this area is strong,
334 and the precipitation is relatively low. The overall performance of CS is that the upper reaches of
335 the Yellow River Basin, the Luohe River Basin, the Fenhe River Basin and the Qinling Mountains
336 are high-value areas of CS. The above-mentioned areas have good vegetation conditions and

337 strong carbon sequestration capacity. The low-value areas are mainly distributed in the Loess
338 Plateau, especially the Mu Us sandy area in the north of the Loess Plateau and the Badain Jaran
339 Desert in the north of the Helan Mountain and in the west of the Yellow River. The basins with
340 higher SC are mainly distributed in the upper reaches of the Yellow River Basin and the central
341 area of the Loess Plateau, especially the upper reaches of the Yellow River, while the SC from
342 Lanzhou to Hekou Town, the Hetao Plain and the lower reaches of the Yellow River is relatively
343 low. The high HQ areas are mainly distributed in the upper river basins and the Taihang
344 Mountains. The main land cover in this area is woodland and grassland. Human activities are
345 infrequent and the level of biodiversity is high. The lower areas are mainly distributed in the
346 Guanzhong Basin, Weihe Valley and the lower Yellow River plain area. This area is a concentrated
347 distribution area of cultivated land and construction land in the Yellow River Basin, highly
348 disturbed by human activities.

349 From the spatial distribution of the five ESs, some show relatively similar spaces, such as HQ
350 and CS, while others show opposite spatial characteristics, such as WY and CS. In short, the five
351 ESs are agglomerated and related in space, rather than randomly distributed with each other.



352

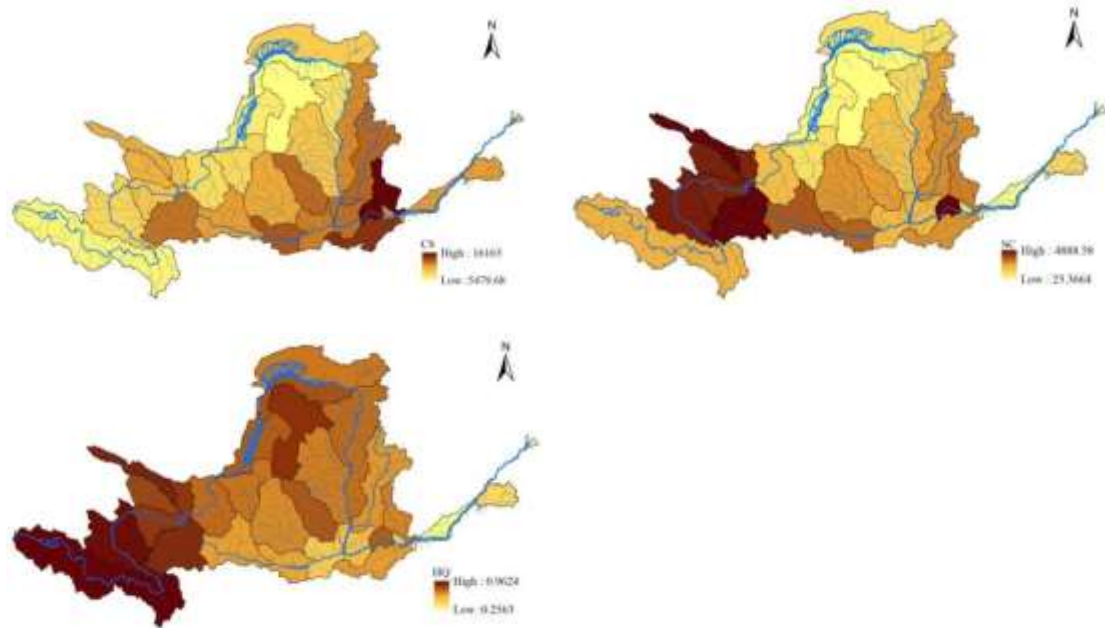
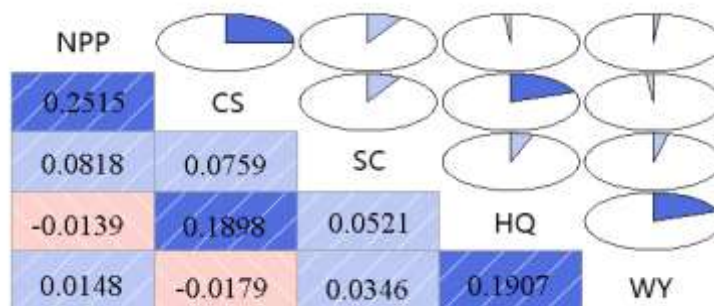


Fig. 2 Spatial distribution map of ESs in the Yellow River Basin

4.2 Trade-off and synergy of ESs in the Yellow River Basin

The correlation between various ESs is shown in the pie chart (Fig. 3). Except for the negative correlation between NPP and HQ, and CS and WY, the correlation coefficients are -0.0139 and -0.0179 respectively, and the other 8 combinations are all positively correlated. The positive correlation between NPP and CS is the strongest ($r=0.2515$), followed by CS and HQ ($r=0.1907$). The results show that NPP has a synergistic relationship with CS, SC, and WY, and a trade-off relationship with HQ. There is a synergistic relationship between CS and SC and HQ, and a trade-off relationship with WY. The relationships between SC and HQ, SC and WY are all synergistic. So is the relationship between HQ and WY.



366

367 **Fig.3** Corrgram of ES pairs in the Yellow River Basin (The values in the lower-left of each
 368 graph are the correlation coefficients of each ES pair in the whole Yellow River Basin)

369 In terms of space(Fig. 4), WY and NPP in the basin are mainly synergistic. The synergy
 370 relationship is particularly prominent in the “Hetao Plain-Ningxia Plain-Lanzhou-Sanmenxia”
 371 area. The rainfall and vegetation coverage is low in the Hetao Plain, Ningxia Hui Autonomous
 372 Region and Lanzhou. In this area, the WY and NPP are relatively low. From Shaanxi to
 373 Sanmenxia, there is abundant rainfall, high WY, and abundant water and heat conditions, which
 374 contributes to the increase of vegetation coverage. The NPP is relatively high. In the Bayan Har
 375 Mountains in the upper reaches of the Yellow River Basin and in Yan'an, Shaanxi and other places
 376 in the middle reaches of the Yellow River Basin, WY and NPP are in a trade-off relationship. The
 377 upstream rainfall is rich and there are permanent glaciers and snowfields, where there is a high
 378 WY. At the same time, there are a large number of grasslands in this area, but the light is
 379 insufficient and the temperature is relatively low, so the NPP is low. While there are woodlands in
 380 Yan'an, Shanxi and other areas with sufficient sunlight, so the NPP is high. Woodlands can
 381 consume a lot of water resources, resulting in low WY in this area, and WY and NPP are in a
 382 trade-off relationship.

383 WY and SC are in a synergistic relationship. The Hetao Plain, Ningxia Plain and

384 Tianshui-Weinan in the middle reaches of the Yellow River Basin show a synergistic relationship.
385 In the Hetao Plain and Ningxia Plain, there is low rainfall, low vegetation coverage, so WY and
386 SC are low. In the Tianshui-Weinan area, there is abundant rainfall, high vegetation coverage, high
387 water production capacity and soil conservation function, while in Huangshui, Taohe and other
388 places, vegetation coverage is high, the consumption of water leads to a decrease in WY, an
389 increase in SC, and below Xiaolangdi in the lower reaches of the Yellow River basin, most of the
390 lands are for construction, and the WY is relatively high. On the contrary, because the area is
391 densely populated, human activities are strong, and vegetation coverage is low, resulting in the
392 decrease of SC, which makes a trade-off relationship between WY and SC.

393 WY and CS show a trade-off relationship throughout the entire region. The two are in a
394 synergistic relationship in a small amount areas of the upper reaches of the Yellow River Basin,
395 the middle reaches of Inner Mongolia, and the Ningxia Hui Autonomous Region. The low
396 precipitation and low vegetation coverage in this area result in low CS and WY. The trade-off
397 relationship is mainly distributed in the upper and middle reaches. In the upper reaches of the
398 Bayan Har Mountains and Zhaling Lake, low-coverage grasslands are mostly distributed, with
399 relatively low CS and high WY. In the middle reaches, such as in Yan'an, Fenhe and Shanxi, there
400 are a large number of woodlands. The higher evapotranspiration and stronger interception capacity
401 of woodland makes the WY of the land smaller. At the same time, the higher carbon density of
402 woodland make the higher CS in this area.

403 WY and HQ show a trade-off relationship. The trade-off relationship and the synergy
404 relationship are interspersed and distributed throughout the basin, and there is no obvious dividing
405 line. The upstream Maqu and the middle Qinling area have high vegetation coverage, strong

406 rainfall, and low-intensity human interference. Therefore, the WY is high and the Q index of
407 habitat quality is high. The Hetao Plain, Ningxia Plain and Guanzhong Plain are located in arid
408 and semi-arid areas with insufficient water and heat conditions, low vegetation coverage, poor
409 water production capacity and habitats, and the two show a synergy relationship. The distribution
410 trade-off relationship is around the synergy relationship, which is mainly distributed in the Mu Us
411 sandy land and below the Xiaolangdi Huayankou in the lower reaches of the Yellow River. The
412 land-use types are unused land and construction land, with less infiltration and large runoff,
413 resulting in higher WY and vegetation. The coverage is low, the downstream population is dense,
414 and human activities are strong, destroying the connectivity of the habitat, resulting in poor HQ.
415 To the west of Lanzhou, the west of Taihang Mountains, they are mostly distributed in
416 high-coverage grassland and woodland due to the high vegetation coverage, which consumes and
417 intercepts a large number of water resources, resulting in a decrease in WY. However, due to its
418 high vegetation coverage, sparse population, and low destructive degree, so HQ is better. WY and
419 HQ are in a trade-off relationship in the above regions.

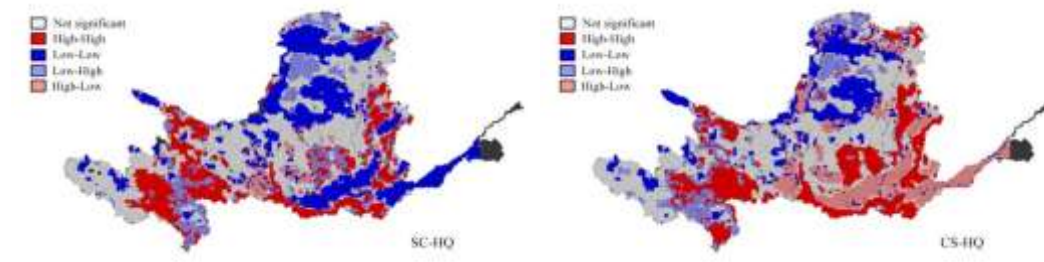
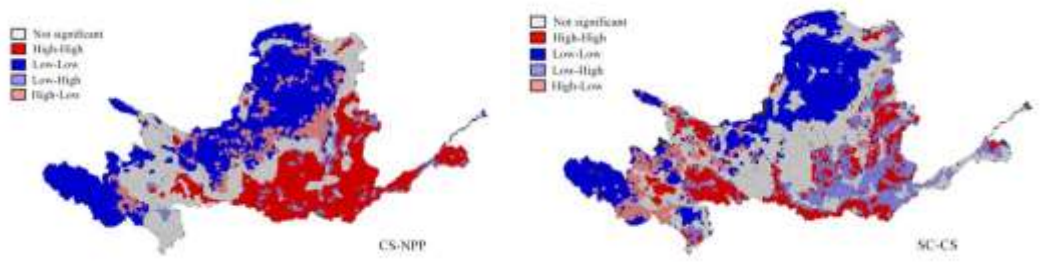
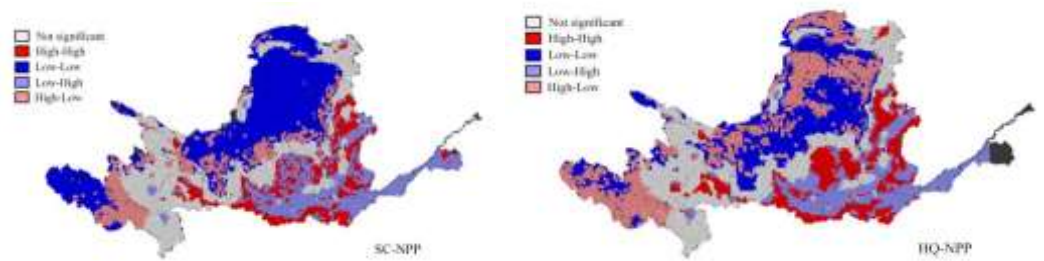
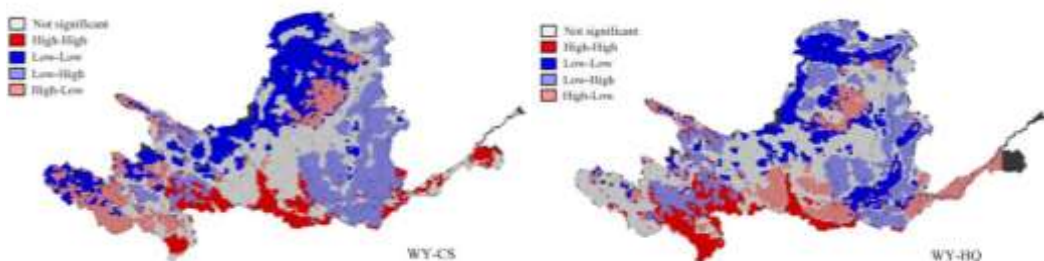
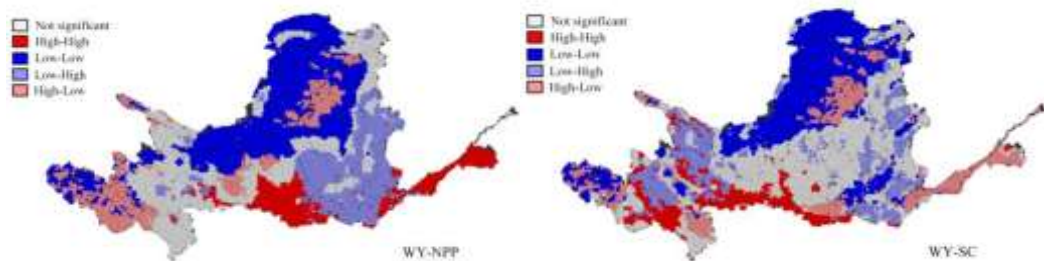
420 NPP and SC are mainly synergistic in the whole region, mainly distributed in the central
421 Qinghai-Tibet Plateau, the northern and southern areas of the Loess Plateau and the lower reaches
422 of the Yellow River Basin. Because of the strong regional dependence of NPP, it will increase with
423 the increase of regional vegetation coverage. The change of coverage changes the resistance to
424 rainfall erosion and indirectly affects the soil retention, so the two maintain consistent changes to a
425 large extent. NPP and CS are also mainly synergistic. From the angle of spatial distribution, the
426 two are synergistic in most areas of the entire basin, and they are distributed throughout the upper
427 and middle reaches of the Yellow River. Obviously, areas with higher vegetation coverage have

428 higher NPP and CS. Compared with the Guanzhong Plain and Taihang Mountains, the upper
429 Bayan Har Mountains, there is lower vegetation coverage in the northern and central parts of the
430 Loess Plateau, so NPP and CS are lower.

431 NPP and HQ are in a synergistic relationship, most of which are distributed in the central
432 Loess Plateau, Yan'an and Shanxi. The central part of the Loess Plateau is dominated by Mu Us's
433 sandy land. The land types are sandy and bare land where the vegetation coverage is low, so NPP
434 and HQ are low. In Yan'an and Shanxi, there is high vegetation coverage, good water and heat
435 conditions, so NPP and HQ are high. However, in the Qinghai-Tibet Plateau and the Loess Plateau,
436 the source area of the Yellow River, there is a trade-off between one and the other. Due to the low
437 degree of human activities in these areas which are far away from threat sources such as cultivated
438 land and construction land, so HQ is high. But NPP is low in these areas due to insufficient light,
439 low temperature and photosynthesis.

440 SC and CS mainly show a synergistic relationship. They are obviously scattered in the middle
441 reaches of the Loess Plateau and Qinling Mountains. The Loess Plateau is mainly concentrated in
442 the Ningxia Hui Autonomous Region and the Mu Us Sandy Land. Due to its lower vegetation
443 coverage and less rainfall, both SC and CS are low in this area. There are many woodlands in the
444 Qinling Mountains, with high vegetation coverage and high carbon density, so SC and CS are high.
445 CS and HQ are mainly synergistic relationship. In the Hetao Plain and the Mu Us Sandy Land, CS
446 and HQ are low due to low vegetation coverage and poor climate conditions. In the Qinling
447 Mountains, Yan'an and Taihang Mountains where woodland is the main land type, the high carbon
448 density, good original vegetation, and low level of damage caused the CS and HQ to change
449 simultaneously. However, in the lower reaches of the Yellow River and the Weihe Valley in the

450 Guanzhong Plain, the land types are mainly woodland, cultivated land and construction land. The
451 flat terrain, frequent human activities, and dense road crossings lead to habitat fragmentation and
452 poor connectivity, resulting in poor HQ. So the two are in a trade-off relationship in these areas.



458 **Fig.4** Schematic diagram of the coordination relationship

459 space of the ESs of the Yellow River Basin

460 4.3 ES bundles

461 The researchers identify the Yellow River Basin ES bundles by using the SOM model. First,
462 they perform a principal component analysis of ESs. The results show that the first two principal
463 components can explain 73% of the total variance of the variables, with WY and HQ having a
464 higher positive load on the first principal component (PC1), NPP and CS having a higher positive
465 load on the second component (PC2), and the load difference of SC on the two principal
466 components is relatively small. From the principal component analysis graph, it can be seen that
467 NPP and CS are relatively close, HQ and WY are relatively close, while NPP and WY tend to be
468 perpendicular, and SC and other ecological services are at a certain distance. Therefore, it is
469 recommended to divide the five ESs into three clusters based on the results of principal
470 component analysis.

471 SOM clustering algorithm has been widely used in the field of environmental science
472 (Václavík et al., 2013). This algorithm can effectively consider the topological relationship
473 between the input data and is of great significance for the division of ES bundles (Cord et al.,
474 2017). The spatial distribution clustering of ESs mainly divided based on the relative similarity of
475 the various services provided by different geographic regions (Renard et al., 2015). Therefore,
476 clustering can directly reflect the spatial differences in the supply level of specific ESs in different
477 regions. According to the spatial distribution and correlation of the five ESs, the Yellow River
478 Basin can be divided into three regions as shown in Fig. 5: The results of the bundles are similar to
479 the upper, middle, and lower basins of the Yellow River Basin, and bundles 1 and 2 is basically

480 bounded by the transition bundles between the Loess Plateau and the Qinghai-Tibet Plateau. On
481 the basis of the ecological function bundles, it obtains the ESs of each ecological function in the
482 district and performs normalization processing by adopting the district statistics means, aiming to
483 analyze each district within the ES structure, and then identifies the active ES function of each
484 district (Fig. 5). According to the result of the division:

485 4.3.1 Bundle 1: the dominate functional area of WY and SC

486 It mainly includes three-level river basins such as Maqu to the source of the river, Maqu to
487 Longyang Gorge, Longyang Gorge to Lanzhou, Daxia River and Tao River, Weihe River and
488 above Baoji Gorge, Huangshui River, and Datong River Basin. The regional area accounts for
489 39.35% of the total area of the Yellow River Basin. WY and SC are significantly higher than that
490 in the other two regions. In this region, there is a plateau mountain climate, affected by the
491 large-scale climate of the Qinghai-Tibet Plateau, with concentrated precipitation, many lakes,
492 grasslands, and swamps, low water consumption and low evapotranspiration. At the same time,
493 vegetation coverage is relatively high, so the conservation services of soil are strong, indicating
494 that the core functions of ESs in this area are WY and SC.

495 4.3.2 Bundle 2: the dominate functional area of HQ and CS

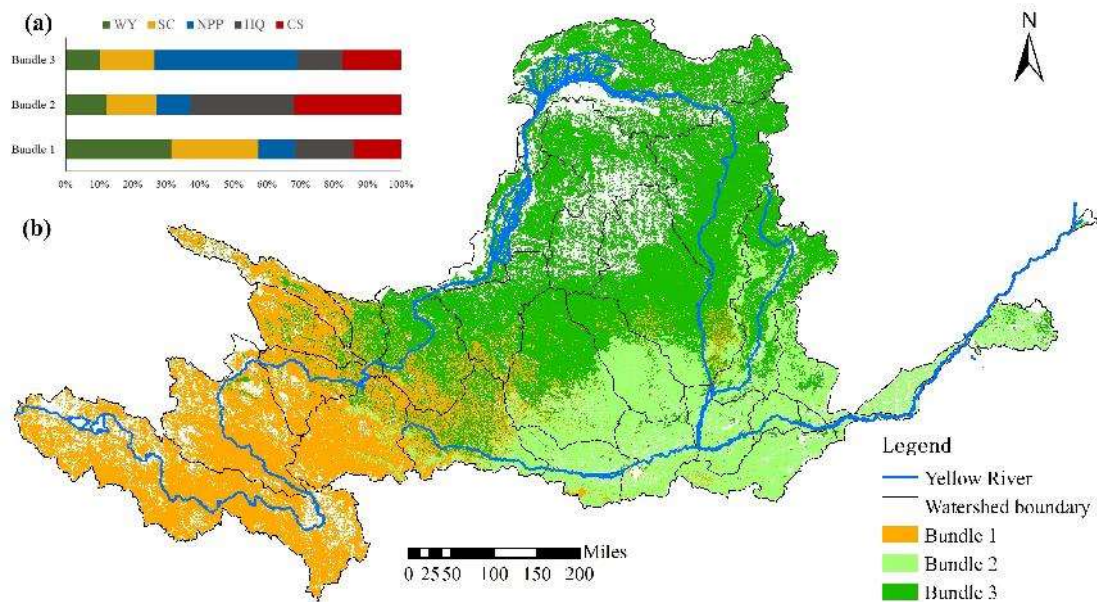
496 It mainly includes three-level river basins such as the Qingshui River and the Kushui River
497 Basin, Xiaheyan to Shizuishan, Shizuishan to the north bank of Hekou Town, Shizuishan to the
498 south bank of Hekou Town, internal flow area, the right bank above Wubao, and the right bank
499 below Wubao. The regional areas account for 35.18% of the total area of the Yellow River Basin.
500 This area is an important functional area for habitat maintenance and carbon storage. There are
501 many types of land use/cover, which mostly are grassland and woodland. However, bare land and

502 sandy land are also distributed in the central area. Due to the large area and the distribution of
503 vegetation types, having high carbon density such as woodland and grassland, the CS is higher. At
504 the same time, due to there is a lower degree of accessibility by human activities in these areas
505 which are also far away from threat sources such as cultivated land and construction land, so HQ
506 is higher than that of in downstream areas. However, the WY service is low and
507 evapotranspiration capacity is strong in the area. It has the largest annual evaporation in the region
508 in this area, which can exceed 2500 mm at most. The insufficient precipitation in the middle
509 reaches leads to the lack and uneven distribution of water resources. In addition, the service
510 function of NPP is also extremely lower than that of other areas. Because this area is located in the
511 hinterland of the inland, it forms a natural landscape with a dominant arid and semi-arid
512 ecosystem. The vegetation structure is simple relatively and the productivity is low in this area
513 which is an extremely poor biomass area in the terrestrial ecosystem of the Yellow River Basin.

514 4.3.3 Bundle 3: the dominate functional area of NPP

515 It distributes in the Fenhe River Basin, the Weihe River from Baoji to Xianyang and below.
516 The regional area accounts for 25.47% of the total area of the Yellow River Basin. Comparing
517 with various ESs, it is found that the NPP service in this area has obvious advantages, so it is the
518 dominant functional area of NPP service. The terrain is relatively flat in these areas, and the
519 mainstream of the Yellow River and many tributaries pass through them. It is a temperate
520 monsoon climate with sufficient water and heat conditions, which is beneficial to vegetation
521 growth and restoration. The woodland coverage is higher in the Qinling Mountains, so the NPP is
522 higher. However, other services are low in this area, especially HQ. Due to the concentrated
523 distribution of arable land and construction land in this area, the habitat is fragmented, the

524 connectivity is reduced, and the distance to the threat factor is relatively small, resulting in low
 525 HQ. The population below Xiaolangdi Huayuankou is dense, the land for economic construction
 526 is concentrated, the vegetation coverage is extremely low, so the SC is small.



527

528 **Fig.5** The spatial distributions of the three ES bundles in Yellow River Basin a.the proportion of
 529 the standardized value of each ES bundle b. the ES bundles map

530 **5. Discussion**

531 Reasonably regulating the time-space trade-offs between multiple services and clarifying
 532 their socio-economic-ecological environment driving mechanism is of great significance to the
 533 sustainable management of the ecosystem and the formulation of land use planning (Tammi et al.,
 534 2017). This paper systematically analyzes the spatial associations of the five important ESs in the
 535 Yellow River Basin and their social-ecological driving mechanism. First, it analyzes the spatial
 536 distribution of the five ESs quantitatively; then compares and analyzes trade-off and synergy
 537 among ESs and their spatial distribution.

538 **5.1 The trade-off and synergy relationship of ESs**

539 Identifying the interrelationships between ESs is essential for understanding services and
540 guiding decision-making (Jiang et al., 2018). However, the interactions between ESs are not all
541 linear. Therefore, the interaction between them can be understood only by evaluating multiple ESs.
542 (Howe et al., 2014). The spatial distribution patterns of the five ESs in the Yellow River Basin are
543 related, and the results are similar to and different from related studies. Supply services and other
544 services usually have a trade-off relationship, especially between agricultural production, water
545 production services and regulation services such as carbon fixation, pollutant retention, and soil
546 conservation (Zhou et al., 2017). The results of this study show that there is a trade-off
547 relationship between WY and CS, but the relationships between water production and SC, HQ and
548 NPP are synergistic. Bennett et al. (2009) believe that the nonlinear relationship between ESs is
549 under the basis of the following two mechanisms: one is driven by common influencing factors;
550 another is the interactions between multiple ESs. Driven by common factors such as rainfall and
551 terrain, there is a synergistic relationship between WY and SC. The increase of NPP can inhibit
552 WY by increasing canopy interception (Wang et al., 2020). HQ, SC and CS are in a spatially
553 synergistic relationship, that is to say, a complete habitat with low interference can offer a superior
554 environment for various organic substances, thereby promoting some adjustment service functions
555 (Peng et al., 2013).

556 This conclusion affirms the support function of HQ, and HQ is in a trade-off relationship
557 with NPP. There are high altitude and low temperature in the places with high HQ, which is not
558 conducive to the photosynthesis of vegetation. In downstream areas with high NPP, frequent
559 human activities lead to lower habitat quality. There is a trade-off relationship between CS and
560 NPP. Although both of these are carbon-related services and share a similar carbon cycle, CS

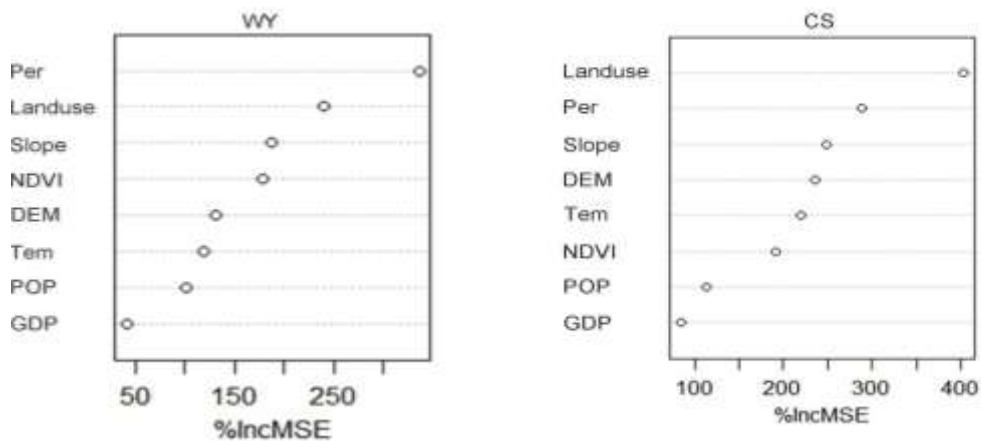
561 represents the stock of carbon and NPP represents the rate of carbon sequestration. There is an
562 opposite relationship between the two. This result is supported by the findings of Zhang et al.
563 (2010). In the Yellow River Basin, there is a wide range of east-west and north-south spans. It is a
564 transitional bundles between the east and the west in our country. The transition has an impact on
565 the barrier and differentiation of the region, resulting in differences in topography, landforms, and
566 climate, which will affect the ecosystem and will promote the difference in ES relationships. The
567 Yellow River Basin spans the Qinghai-Tibet Plateau, the Inner Mongolia Plateau, the Loess
568 Plateau and the Huanghuaihai Plain from the west to the east. The height difference between the
569 east and the west is huge, and the climate of different regions is obviously different. The Yellow
570 River Basin is mainly in the southern temperate bundles, middle temperate bundles and plateau
571 climate bundles. These differences make the vegetation, soil, animals and plants in the Yellow
572 River Basin show significant latitude zonality differences, longitude differentiation, and natural
573 rules such as vertical zonality and slope differentiation, which promote the high complexity and
574 diversity of ESs in the Yellow River Basin, and more importantly, promote the spatial
575 heterogeneity.

576 5.2 Factors affecting the spatial distribution of ESs

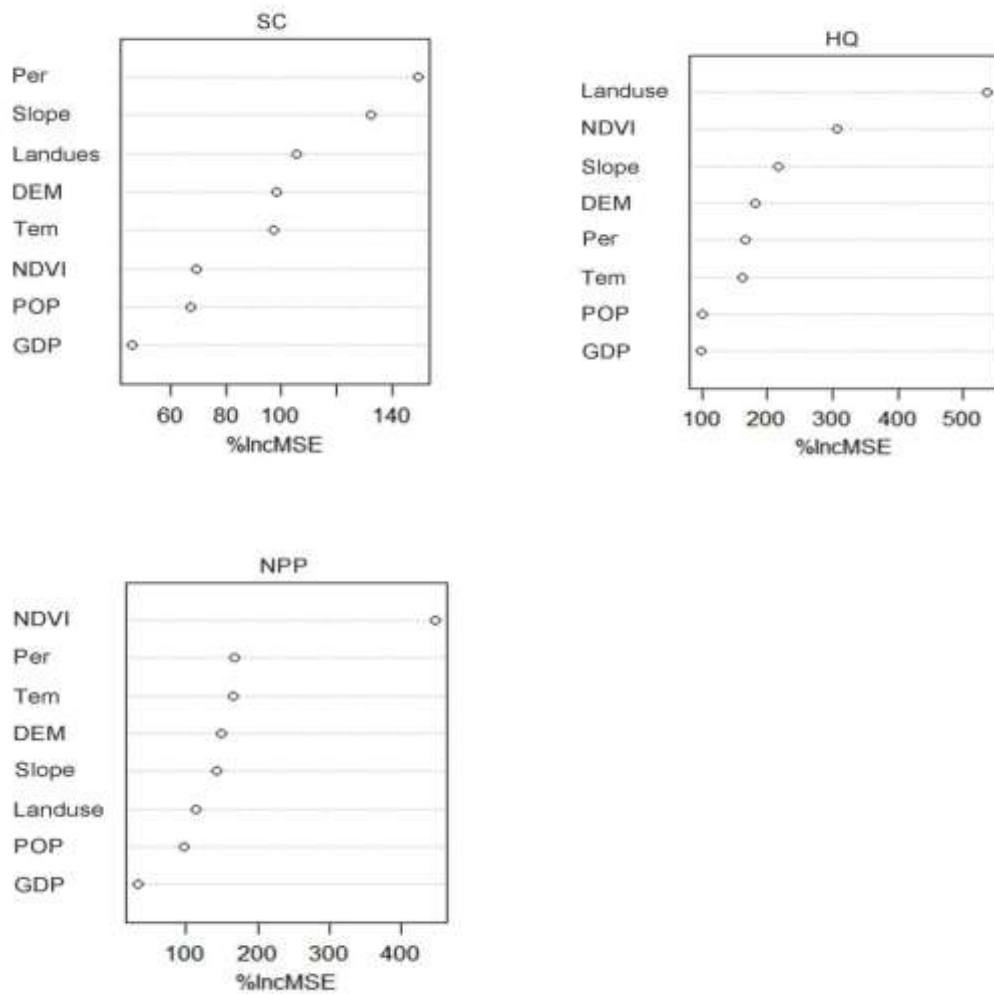
577 It performs statistical modeling on the social-ecological environmental factors of the five ESs
578 in the Yellow River Basin in 2018 by using the random forest regression model. The fitting
579 degrees are all above 0.90, indicating that the model can well fit the spatial distribution differences
580 of ESs. The relative weights of the eight environmental factors on the spatial distribution of the
581 five ESs are shown in Fig. 6: WY is affected by climatic factors more, especially precipitation,
582 which has consistence with the results of previous studies (Yang et al., 2019). WY is the result of

583 comprehensive consideration of the balance of harvest (precipitation) and support (actual
584 evapotranspiration) during the regional water cycle. Therefore, WY is not only greatly affected by
585 rainfall, but also affected by the actual evapotranspiration in the region. The actual
586 evapotranspiration is not only affected by weather factors (temperature, wind speed, relative
587 humidity and sunshine hours, etc.), it is also affected directly by the land use/cover of the
588 underlying surface. The land use impact on actual evapotranspiration is mainly through changing
589 the underlying surface conditions, thereby affecting WY (Lang et al., 2018). SC is mainly affected
590 by rainfall, because precipitation is one of the leading factors that cause soil erosion. The increase
591 in precipitation leads to intensified soil erosion, which leads to a decrease in soil conservation (Liu
592 et al., 2018). The results show that slope is also one of the important factors affecting SC, because
593 there is a less human disturbance, higher vegetation coverage, lower actual erosion, and larger soil
594 conservation in the steep slope area (EI et al., 2013). In the plain area of the lower Yellow River,
595 despite the heavy rainfall, flat terrain, and small vegetation coverage, the actual erosion amount is
596 also large, so the SC is small, and other factors have no obvious impact on the SC. Land use type
597 is the most important factor affecting CS. From the perspective of the spatial distribution of CS,
598 the upper reaches of the Yellow River Basin, Luohe River Basin, Fenhe River Basin and Qinling
599 Mountains are the high-value areas of CS, which are mainly woodland and high-coverage
600 grassland, with good vegetation conditions and strong carbon sequestration capacity. The
601 low-value of CS areas are mainly distributed in the Loess Plateau, especially the Mu Us sandy
602 area in the north of the Loess Plateau and the Badain Jaran Desert in the north of the Helan
603 Mountain and in the west of the Yellow River, which is mainly sandy and other unused lands. At
604 the same time, the influence of temperature on CS is more important than other factors. This

605 conclusion is consistent with the results of Zhao et al. (2018), because the vegetation is easier to
606 recover in areas with high temperatures. The spatial distribution of HQ is absolutely affected by
607 the types of land use. The HQ of the Yellow River Basin as a whole presents the spatial
608 characteristics of high in the west and low in the east, mainly because the upstream is dominated
609 by woodland and grassland, while the cultivated land is concentrated in the downstream area. This
610 is consistent with the researches in other regions at home and abroad. (Ma et al., 2019; Brumm et
611 al., 2019; Yang et al., 2017). At the same time, natural features such as topography, climate, and
612 NDVI are stable endogenous driving factors relatively, which determine the HQ spatial
613 distribution, while social economic activities considered as manageable external driving factors
614 often lead to the degradation of HQ (Yan et al., 2018). The influence of NDVI on NPP is much
615 higher than other factors. The spatial distribution of NPP and NDVI tends to be consistent. Due to
616 the sensitivity of NDVI to ground vegetation chlorophyll changes and high temporal and spatial
617 resolution, it can sensitively reflect the dynamic changes of NPP (Jiang et al., 2011).



618



619

620

621 **Fig. 6** Impact factors and degree of impact of various ESs(Per:precipitation, Tem:temperature,
 622 POP:population density, GDP:gross domestic product)

623 **5.3 Land use management implications**

624 Because the spatial heterogeneity of ESs determines different ES combinations, zoning can
 625 quickly identify areas with similar ecosystem clusters determined by similar social environment
 626 and other factors, so that policies can better formulate sustainable development strategies for
 627 different regions (Hamann et al., 2015). At the same time, ESs are affected by land-use ways and
 628 patterns, but most studies show that land-use types have the greatest impact on ESs (Paterson et al.,
 629 2012). Therefore, policy makers must understand how to construct land-use structures in a more

630 reasonable way to promote regional sustainable development. Based on the bundles results of the
631 Yellow River Basin, they put forward several suggestions for the future urbanization and land
632 planning in different areas. In bundle 1, multiple ESs are superimposed here, with irreplaceable
633 ecological functions. In future, it should be strictly managed as a key protected ecological function
634 area, delineate the ecological protection red line, and strictly enforce the ecological access system.
635 It is strictly forbidden to carry out various development activities that do not conform to the main
636 function positioning in the area designated as the ecological protection red line. It is necessary to
637 promote ecological protection, restoration and construction projects with grassland restoration as
638 the main body, focusing on the Three Rivers, Qilian Mountains, and the upper reaches of the
639 Yellow River in Gannan, so as to improve the authenticity and integrity of the ecosystem. In terms
640 of implementation measures, the researchers adhere to the principle of ecological priority and
641 organic integration of production and ecology. Grassland pastures such as Gannan Plateau should
642 carry out ecological restoration, strictly implement grass-determining livestock, control livestock
643 carrying capacity, fundamentally curb overloading and overgrazing, and remove part of the
644 ecological system and carrying capacity to wild animals, and establish and improve a natural
645 reserve system with national parks as the main body. Management measures such as the
646 prohibition of grazing, rest grazing, reduction of grazing, and rotation of grazing should be taken
647 to accelerate the restoration of degraded grasslands. Measures such as reseeded of native grass
648 seeds and soil bioremediation should be adopted to accelerate the restoration and reconstruction of
649 severely degraded grasslands, strengthen the protection of biodiversity, ensure the connectivity of
650 habitat, and improve environmental carrying capacity and water conservation capacity. In bundle 2,
651 it encompasses the entire Loess Plateau. In this area, there is not only low rainfall and uneven

652 distribution, but also heavy rainstorms, coupled with the loose structure of loess, so it is easy to
653 form soil erosion. From 1950, our country began to adopt measures such as slope management,
654 joint management of slope and gully, comprehensive consolidation of small watersheds, and
655 returning farmland to forests and grasslands to control serious soil erosion problems in this area.
656 In general, the currently implemented soil erosion control measures and projects in the Loess
657 Plateau have achieved significant ecological benefits, and the overall regional ESs have developed
658 in a healthy direction; however, the overall fragile characteristics of the Loess Plateau's ecological
659 environment have not been changed. Therefore, people should not only consider reducing soil
660 erosion and increasing the area of arable land for the management of this area, more importantly,
661 they should also improve landscape varieties and the living environment, optimize the economic
662 and industrial structure, and boost regional social and economic growth. Guided by the concept of
663 landscape, forests, fields, lakes and grasses as a living community, people should practice the
664 idea of “reinforcing the ditch and protecting the plateau in plateau areas, returning farmland to
665 forests and grasses on slopes, blocking trenches for land preparation, and fixing sand and restoring
666 shrubs and grasses in sandy areas”. A comprehensive protection system for the plateau and ditch
667 head with water systems and roads as the framework of fields, roads, forests, villages, shelter
668 forests, etc. on the plateau and ditch should be formed to prevent the development of erosion ditch
669 on the plateau. A ditch slope protection system that focuses on vegetation restoration, and
670 combines engineering measures with forest, grass, and plant measures on the sloped surface is
671 formed to reduce the water erosion of the ditch slope. The Saying Gully Scouring Forest has
672 formed a gully protection system combining trench engineering and forest, grass and vegetation
673 measures to prevent gravitational erosion such as collapses, landslides, and gully bank expansion.

674 In bundle 3, it is a densely populated area with concentrated construction land. The disorderly and
675 intensive urbanization process and agricultural development in this area are the main reasons for
676 the loss of other important ESs. This is consistent with the results of other areas (Cumming et al.,
677 2014; Seto et al., 2012; Foley et al., 2011). The expansion of cities has led to the reduction of the
678 service functions of CS, HQ, and SC. The ESs in urban concentrated areas are mainly reflected in
679 green infrastructure. Therefore, in urban core areas, it establishes the green belts to eliminate the
680 side effects of increased impervious surfaces, taking into account the low contribution rate of
681 unused land to ESs. Therefore, priority is given to unused land in site selection for new
682 urbanization.

683 **6. Conclusion**

684 This study evaluated the five ESs of the Yellow River Basin in 2018, including WY, CS, SC,
685 HQ, and NPP, and made a spatial expression with the three-level basin as a unit, and then
686 quantitatively analyzed the trade-offs and synergies among the five ESs. It delineated the
687 dominant ecological service function bundles of the Yellow River Basin based on the SOM
688 method. The main conclusions are as follows:

689 The spatial distribution of the 5 ESs not only shows spatial heterogeneity, but also reflects
690 certain regional laws. The upper reaches of the basin show higher ES, especially WY, SC and HQ
691 are significantly higher than that of in the middle reaches and lower reaches of the Yellow River
692 basin, however ESs is generally lower in the middle reaches.

693 NPP has a synergistic relationship with CS, SC, and WY, and a trade-off relationship with
694 HQ. CS has a synergistic relationship with SC and HQ, and a trade-off relationship with WY. The
695 trade-off synergy relationship shows obvious spatial heterogeneity in space. The vegetation, soil,

696 animals and plants in the Yellow River Basin all show significant latitude zonality differences,
697 longitude differentiation, and natural laws such as vertical zonality and slope differentiation,
698 which promotes the high complexity and diversity of ESs in the Yellow River Basin, more
699 importantly, promotes the heterogeneity of space.

700 According to the spatial distribution and related relationships of the five ESs, the dominant
701 ecological function services in the Yellow River Basin can be divided into 3 bundles. Bundle 1 is
702 the dominant function area for WY and SC services, Bundle 2 is the dominant function area for
703 HQ and CS services, and Bundle 3 is the NPP service dominate function area.

704 **Acknowledgments**

705 This study was financed by the National Key R&D Program of China (No.
706 2016YFC0501902)

707 **Conflicts of Interest**

708 The authors declare no conflict of interest.

709

710

711 **References**

712 Bao, Y.B., Liu, K., Li, T., Hu, S., 2015. Effects of land use change on habitat based on InVEST
713 model-taking Yellow River wetland nature reserve in Shaanxi province as an example. *Arid*
714 *Zone Research*. 32(3): 622-629.10.13866/j.azr. 2015.03.29

715 Baro, F., Gomez-Baggethun, E., Haase, D., 2017. Ecosystem service bundles along the urban-rural
716 gradient: Insights for landscape planning and management. *Ecosystem Services*, 24, 147-159.
717 10.1016/j.ecoser.2017.02.021.

718 Bennett, E.M., Peterson, G.D., Gordon, L.J., 2009. Understanding relationships among multiple
719 ecosystem services. *Ecol. Lett.* 12, 1394-1404.10.1111/j.1461-0248.2009.01387.x.

720 Brumm, K.J., Jonas, J.L., Prichard, C.G., Watson, N.M., Pangle, K.L., 2019. Land cover
721 influences on juvenile Rainbow Trout diet composition and condition in Lake Michigan
722 tributaries. *Ecol. Freshw. Fish.* 28, 11-19. 10.1111/eff.12422

723 Chen, L.J., Liu, G.H., Li, H.G., 2002. Remote sensing dynamic monitoring of net primary
724 productivity of vegetation in China. *Journal of Remote Sensing*, 6(2): 129-136.1007-4619
725 (2002)02-0129-07.

726 Chen, Q., Chen, Y.H., Wang, M.J., Jiang, W.G., Hou, P., Li, Y., 2014. Analysis on the change of
727 net primary productivity of vegetation and the driving factors of climate in the Yellow River
728 Basin from 2001 to 2010. *Chinese Journal of Applied Ecology.* 25(10):
729 2811-2818.10.13287/j.1001-9332.20140731.003。

730 Cheng, G.D., Li, X., 2015. Watershed science and its integrated research methods . *Chinese*
731 *science: Earth science*, 45(6): 811-819.

732 Chuai, X.H., Huang, X.J., Lai, L., Wang, W.J., Peng, J.W., Zhao, R.Q., 2013. Land use structure
733 optimization based on carbon storage in several regional terrestrial ecosystems across China.
734 *Environmental Science and Policy*, 25. 10.1016/j.envsci.2012.05.005

735 Cord, A.F., Brauman, K.A., Chaplin-Kramer, R., Huth, A., Ziv, G., Seppelt, R., 2017. Priorities to
736 advance monitoring of ecosystem services using earth observation. *Trends Ecol. Evol.* 32,
737 416e428. 10.1016/j.tree.2017.03.003.

738 Costanza, R., de Groot, R., Braat, L., Kubiszewski, I., Fioramonti, L., Sutton, P., et al. 2017.
739 Twenty years of ecosystem services: How far have we come and how far do we still need to
740 go? *Ecosystem Services*, 28, 1-16. 10.1016/j.ecoser.2017.09.008.;

741 Cumming, G.S., Buerkert, A., Hoffmann, E.M., Schlecht, E., von Cramon-Taubadel, S.,
742 Tschardtke, T., 2014. Implications of agricultural transitions and urbanization for ecosystem
743 services. *Nature.* 515, 50–57. 10.1038/nature13945.

744 Deng, X., Li, Z., Gibson, J., 2016. A review on trade-off analysis of ecosystem services for
745 sustainable land-use management. *Journal of Geographical Sciences*, 26(7), 953-968.
746 10.1007/s11442-016-1309-9.

747 El, K.H., Zhang, H., Zhang, P.C., Mosandl, R., 2013. Soil erosion and surface runoff on different
748 vegetation covers and slope gradients: A field experiment in Southern Shaanxi Province,

749 China. *Catena*.105: 1-10.1016/j.catena.2012.12.012.

750 Foley, J.A., Ramankutty, N., Brauman, K.A., Cassidy, E.S., Gerber, J.S., Johnston, M., et al. 2011.

751 Solutions for a cultivated planet. *Nature*, 478, 337-342.

752 Fu, B.J., Yu, D.D., 2016. Trade-off analyses and synthetic integrated method of multiple

753 ecosystem services. *Resources Science*, 38(01): 0001-0009.10.18402/resci.2016.01.01

754 Fu, B.J., Zhang, L.W., 2014. Land-use change and ecosystem services: concepts, methods and

755 progress. *Progress in Geography*, 33(04): 441-446.10.11820/dlkxjz.2014.04.001

756 Hamann, M., Biggs, R., Reyers, B., 2015. Mapping social-ecological systems: Identifying

757 'green-loop' and 'red-loop' dynamics based on characteristic bundles of ecosystem service

758 use. *Global Environ. Change*, 34, 218-226.10.1016/j.gloenvcha.2015.07.008.

759 Hou, Y., Lu, Y.H., Chen, W.P., Fu, B.J., 2017. Temporal variation and spatial scale dependency of

760 ecosystem service interactions: a case study on the central Loess Plateau of China.

761 *Landscape Ecology*, 32 (6): 1201-1217. 10.1007/s10980-017-0497-8.

762 Howe, C., Suich, H., Vira, B., Mace, G.M., 2014. Creating win-wins from trade-offs? Ecosystem

763 services for human well-being: A meta-analysis of ecosystem service trade-offs and synergies

764 in the real world. *Global Environmental Change*, 28, 263-275.

765 10.1016/j.gloenvcha.2014.07.005.

766 Hu, X., Hong, W., Qiu, R., Hong, T., Chen, C., Wu, C., 2015. Geographic variations of ecosystem

767 service intensity in Fuzhou City, China. *Science of The Total Environment*. 512-513,

768 215-226. 10.1016/j.scitotenv.2015.01.035.

769 Jiang, C., Li, D., Wang, D., Zhang, L., 2016. Quantification and assessment of changes in

770 ecosystem service in the Three-River Headwaters Region, China as a result of climate

771 variability and land cover change. *Ecological Indicators*, 66, 199-211.

772 10.1016/j.ecolind.2016.01.051.

773 Jiang, C., Zhang, H., Zhang, Z., 2018. Spatially explicit assessment of ecosystem services in

774 China's Loess Plateau: Patterns, interactions, drivers, and implications. *Global Planet.*

775 *Change*. 161, 41–52. 10.1016/j.gloplacha. 2017.11.014.

776 Jiang, R.Z., Li, X.Q., Zhu, Y.A., Zhang, Z.G., 2011. Spatial-temporal variation of NPP and NDVI

777 correlation in wetland of Yellow River Delta based on MODIS data. *Acta Ecologica Sinica*.

778 31(22) : 6708-6716

779 Kohonen, T., Makisara, K., 1989. The Self-Organizing Feature Maps. *Physica Scripta*, 9 (1):
780 168-172.

781 Lang, Y.Q., Song, W., Deng, X.Z., 2018. Projected land use changes impacts on water yields in the
782 karst mountain areas of China. *Physics and Chemistry of the Earth*. 104:
783 66-75.10.1016/j.pce.2017.11.001.

784 Li, J., Li, H.L., Zhang, L., 2016. Ecosystem service trade-offs in the Guanzhong-Tianshui
785 economic region of China. *Acta Ecologica Sinica*, 36(10): 3053-3062.10.5846
786 /stxb201408261688

787 Li, K.R., Wang, S.Q., Cao, M.K., 2002. Carbon storage of vegetation and soil in China. *Science*
788 *China*. 33(1): 72-80

789 Li, Y. J., Zhang, L.W., Qiu, J. X., Yan, J. P., Wan, L. W., Wang, P. T., et al. 2017. Spatially explicit
790 quantification of the interactions among ecosystem services. *Landscape Ecology*, 32 (6),
791 1181-1199. 10.1007/s10980-017-0527-6.

792 Liu, C.Y., Zhu, K.W., Liu, J.P., 2017. Evolution and prediction of land cover and biodiversity
793 function in Chongqing section of Three Gorges Reservoir Area. *Transactions of the Chinese*
794 *Society of Agricultural Engineering (Transactions of the CSAE)*. 33(19): 258-267

795 Liu, D.Q., Gong, J., Zhang, J.Q., Ma, X.C., 2018. Spatiotemporal variation of soil conservation
796 function and its influencing factors in Bailongjiang Watershed in Gansu Province. *Research*
797 *of Soil and Water Conservation*, 25(4): 94-103.10.31497/zrzyxb.20200716

798 Liu, Y., Bi, J., Lü, J.S., 2019. Trade-off and synergy relationships of ecosystem services and the
799 driving forces: a case study of the Taihu Basin, Jiangsu Province. *Acta Ecologica Sinica*.
800 39(19):7067-7078. 10.5846 /stxb201808091690

801 Lyu, R.F., Zhang, J.M., Xu, M.Q., Li, J.J., 2018. Impacts of urbanization on ecosystem services
802 and their temporal relations: A case study in Northern Ningxia, China, *Land Use Policy*,
803 77:163-173.10.1016/j.landusepol.2018.05.022.

804 Ma, L.B., Bo, J., Li, X.Y., Fang, F., Cheng, W.J., 2019. Identifying key landscape pattern indices
805 influencing the ecological security of inland river basin: The middle and lower reaches of
806 Shule River Basin as an example. *Sci. Total Environ.* 674,

807 424-438.10.1016/j.scitotenv.2019.04.107

808 MEA, 2005a. Ecosystems and Human Well-being: Current State and Trend: Synthesis. Island
809 Press, Washington DC

810 Mouchet, M. A., Lamarque, P., Martín-López, B., Crouzat, E., Gos, P., Byczek, C., et al. 2014. An
811 interdisciplinary methodological guide for quantifying associations between
812 ecosystem services. *Global Environmental Change*, 28, 298-308.
813 10.1016/j.gloenvcha.2014.07.012

814 Mu, S.J., Li, J.L., Zhou, W., Yang, H. F., Zhang, C.B., Ju, W.M., 2013, Spatial-temporal
815 distribution of net primary productivity and its relationship with climate factors in Inner
816 Mongolia from 2001 to 2010. *Acta Ecologica Sinica*. 33(12) : 3752-3764.10.5846
817 /stxb201205030638.

818 Paterson, A., Bryan, B.A., 2012. Food-carbon trade-offs between agriculture and reforestation
819 land uses under alternate market-based policies. *Ecol. Soc.* 17, 21.10.5751/es-04959-170321

820 Peng, Y.X., Wu, J.Z., Luan, Z.P., Feng, L., 2013. Evaluation of biodiversity in typical forest
821 ecosystems in China: a review. *For. Eng.* 29, 4-10 .10.16270/j.cnki.slgc.2013.06.046

822 Piao, S.L., Fang, J.Y., Guo, Q.H., 2001. Application of CASA model to the estimation of Chinese
823 terrestrial net primary productivity. *Acta Phytocologica Sinica*. 25(5): 603-608.

824 Richards, D.R., Friess, D.A., 2017. Characterizing coastal ecosystem service trade-offs with future
825 urban development in a tropical city. *Environmental Management*, 60(5): 961-973.
826 10.1007/s00267-017-0924-2.

827 Rositano, F., Bert, F.E., Piñeiro, G., Ferraro, D.O., 2017. Identifying the factors that determine
828 ecosystem services provision in Pampean agroecosystems (Argentina) using a data-mining
829 approach. *Environmental Development*. 25, 3-11. 10.1016/j.envdev.2017.11.003

830 Seto, K.C., G.ernalp, B., Hutyra, L.R., 2012. Global forecasts of urban expansion to 2030 and
831 direct impacts on biodiversity and carbon pools. *Proc. Natl. Acad. Sci. USA*. 109,
832 16083-16088. 10.2307/41763206.

833 Sharp, R., Tallis, H., Ricketts, T., Guerry, A., Wood, S.A., Chaplin-Kramer, R., Nelson, E., 2018.
834 InVEST 3.6.0 User's Guide. The Natural Capital Project. Stanford university, University of
835 Minnesota, The Nature Conservancy, and World Wildlife Fund.

836 Song, W., Deng, X.Z., 2017. Land-use/Land-cover change and ecosystem service provision in
837 China. *Science of the Total Environment*, 576:705-719.10.1016/j.scitotenv.2016.07.078

838 Sun, Y.J., Ren, Z.Y., Hao, M.Y., Duan, Y.F., 2019, Spatial and temporal changes in the synergy and
839 trade-off between ecosystem services, and its influencing factors in Yanan, Loess Plateau.
840 *Acta Ecologica Sinica*, 39(10): 3443-3454.10. 5846 /stxb201808141730

841 Tammi, I., Mustajärvi, K., Rasinmäki, J., 2017. Integrating spatial valuation of ecosystem services
842 into regional planning and development. *Ecosystem Services*. 26, 329-344.
843 10.1016/j.ecoser.2016.11.008.

844 Tolessa, T., Senbeta, F., Kidane, M., 2017, The impact of land use/land cover change on ecosystem
845 services in the central highlands of Ethiopia. *Ecosystem Services*, 23: 47-54.
846 10.1016/j.ecoser.2016.11.010

847 Trodahl, M.I., Jackson, B.M., Deslippe, J.R., Metherell, A.K., 2017, Investigating trade-offs
848 between water quality and agricultural productivity using the Land Utilisation and Capability
849 Indicator (LUCI)-A New Zealand application. *Ecosystem Services*, 26:
850 388-399. 10.1016/j.ecoser.2016.10.013

851 Wang, B., Zhao, J., Hu X.F., 2018. Analysis on trade-offs and synergistic relationships among
852 multiple ecosystem services in the Shiyang River Basin. *Acta Ecologica Sinica*, 38(21):
853 7582-7595.10.5846/stxb201711272126.

854 Wang, Y.H., Dai, E. F., 2020. Spatial-temporal changes in ecosystem services and the trade-off
855 relationship in mountain regions: A case study of Hengduan Mountain region in Southwest
856 China, *Journal of Cleaner Production*, 264, 10.1016/j.jclepro.2020.121573.

857 Wu, X., Liu, S., Zhao, S., Hou, X., Xu, J., Dong, S., et al. 2019. Quantification and driving force
858 analysis of ecosystem services supply, demand and balance in China. *Sci Total Environ*, 652,
859 1375-1386. 10.1016/j.scitotenv. 2018 .10.329.

860 Xie, X.L., Sun, B., Zhou, H.Z., Li, Z.P., Li, A.B., 2004. Estimation and spatial distribution of soil
861 organic carbon density and storage in China. *Acta Pedologica Sinica* , 41(1): 35-43

862 Yan, S.J., Wang, X., Cai, Y.P., Li, C.H., Yan, R., Cui, G.N., Yang, Z.F., 2018. An integrated
863 investigation of spatiotemporal habitat quality dynamics and driving forces in the upper basin
864 of miyun reservoir North China. *Sustainability*. 10 (12), 4625–4641.10.3390/su10124625.

865 Yang, D., Liu, W., Tang, L.Y., Chen, L., Li, X.Z., Xu, X.L., 2019. Estimation of water provision
866 services for monsoon catchments of South China: Applicability of the InVEST model.
867 *Landscape and Urban Planning*. 182: 133-143.10.1016/j. landurbplan.2018.10.011

868 Yang, J., Xie, B.P., Zhang, D.G., 2020. Spatio-temporal variation of water yield and its response to
869 precipitation and land use change in the Yellow River Basin based on InVEST model.
870 *Chinese Journal of Applied Ecology*. 31(08):2731-2739. 10.13287 /j.1001-9332.202008.015.

871 Yang,W., Jin, Y., Sun, T., Yang, Z., Cai, Y., Yi, Y., 2017. Trade-offs among ecosystem services in
872 coastal wetlands under the effects of reclamation activities. *Ecol. Indic.* 92,
873 354-366.10.1016/j.ecolind.2017.05.005.

874 Ying, H., Zhang, H.Y., Zhao, J.J., Shan, Y., Zhang, Z.X., Guo, X.Y., et al. 2020, Effects of spring
875 and summer extreme climate events on the autumn phenology of different vegetation types of
876 Inner Mongolia, China, from 1982 to 2015. *Ecological Indicators*, 111.
877 10.1016/j.ecolind.2019.105974.

878 Zhang, L., Dawes, W.R., Walker, G.R., 2001. Response of mean annual evapotranspiration to
879 vegetation changes at catch-ment scale. *Water Resources Research*, 37(3):
880 701-708.10.1029/2000WR900325.

881 Zhang, P., Zhang, Y., Yang, G., Zheng, Z., Liu, Y., Tan, Z., 2010. Carbon storage and sequestration
882 of tree layer in subtropical evergreen broadleaf forests in Ailao Mountain of Yunnan. *Chin. J.*
883 *Ecol.* 29, 1047-1053.10.3724/SP. J.1035.2010.01150

884 Zhang, X.R., Zhou, J., Li, G.N., et al. 2020. Spatial pattern reconstruction of regional habitat
885 quality based on the simulation of land use changes from 1975 to 2010. *Journal of*
886 *Geographical Sciences*, 30(12): 601-620.10.1007/s1 1442-020-1745-4.

887 Zhao, M.M., He, Z.B., Du, J., Chen, L.F., Lin, P.F., Fang,S., 2018. Assessing the effects of
888 ecological engineering on carbon storage by linking the CA-Markov and InVEST models.
889 *Ecological Indicators*, 98(MAR.):29-38.10.1016/j.ecolind. 2018.10.052

890 Zhong, L.N., Wang, J., 2017. Evaluation on effect of land consolidation on habitat quality based
891 on InVEST model. *Transactions of the Chinese Society of Agricultural Engineering*
892 (Transactions of the CSAE). 33(1): 250-255.

893 Zhou, Z.X., Li, J., 2015. The correlation analysis on the landscape pattern index and hydrological

894 processes in the Yanhe watershed, China. *Journal of Hydrology*, 524, 417-426.
895 10.1016/j.jhydrol.2015.02.028.

896 Zhou, Z.X., Li, J., Guo, Z.Z., Li, T., 2017. Trade-offs between carbon, water, soil and food in
897 Guanzhong-Tianshui economic region from remotely sensed data. *International Journal of*
898 *Applied Earth Observation and Geoinformation*, 58, 145-156. 10.1016/j.jag.2017.01.003.

899 Zhu, W.Q., Chen, Y.H., Xu, D., Li, J., 2005a. Advances in terrestrial net primary productivity
900 (NPP) estimation models. *Chinese Journal of Ecology*. 24(3) :296-300. 10.13292/j .1000
901 -4890.2005.0256

902 Zhu, W.Q., Pan, Y.Z., Long, Z.H., Chen, Y.H., Li, J., Hu, H.B., 2005b. Estimating net primary
903 productivity of terrestrial vegetation based on GIS and RS: a case study in Inner Mongolia,
904 China. *National Remote Sensing Bulletin*. 2005b. 3(9): 300-307. 1007-4619(2005)
905 03-0300-08

906 Zoderer, B.M., Tasser, E., Erb, K.H., Lupo Stanghellini, P.S., Tappeiner, U., 2016. Identifying and
907 mapping the tourists perception of cultural ecosystem services: A case study from an Alpine
908 region. *Land Use Policy*, 56, 251-261. 10.1016/j.landusepol.2016.05.004.